

MWM[®]-Array Inspection for Quality Control of Friction Stir Welded Extrusions

David Grundy, Vladimir Zilberstein, and Neil Goldfine

JENTEK Sensors, Inc., Waltham, MA, USA

Phone: (781) 642-9666, Fax: (781) 642-7525; email: jentek@shore.net

Jerrold Green and Israel Stol

Alcoa Technical Center, Pittsburgh, PA, USA

Abstract

For several years, Alcoa has been actively involved in developing aluminum alloys and joining techniques for the aerospace industry. As part of its effort to identify and acquire effective non-destructive inspection techniques for the presence of discrepant discontinuities at the back side of Friction Stir Welds (FSW), Alcoa has contracted JENTEK Sensors Inc. to test and demonstrate JENTEK's eddy current based methods for detection of such discontinuities. This paper describes methods for the detection of discrepant conditions, i.e., discontinuities, including lack of penetration (LOP) and kissing bonds (KB) in Friction Stir Welds (U.S. patents issued¹ and pending). Results presented here for FSW joints in aluminum alloy extrusions demonstrate the capability of eddy current sensors, such as Meandering Winding Magnetometer array sensors (MWM[®]-Arrays), to inspect the FSWs for discontinuities and reveal different regions with distinct microstructures, e.g., dynamically recrystallized zone (DXZ), thermomechanically-affected zone (TMAZ) and heat-affected zone (HAZ) in such welds. MWM-Array generated images of electrical conductivity and feature recognition and characterization of local transverse variations in electrical conductivity are used to reveal and detect discontinuities such as LOP and KB from microstructural variations in the FSW butt joints. This capability to reveal microstructural variations in FSWs was used for estimation of the LOP depth in square butt joints as reported at the 2002 Trends in Welding Research Conference.²

Introduction

The objective of this study was to demonstrate detection of KB and LOP on the backside of FSW butt joints intended for use in aircraft structures. The FSW process, invented and licensed by TWI in Cambridge, UK, in the early nineties³ is fast becoming a process of choice for a variety of structural applications. This solid state joining process has numerous advantages over fusion welding including fewer discrepant conditions and comparable or better mechanical properties. Quality requirements for FSW in aircraft structures operating under cyclical loads are very stringent. It is critical to avoid any preexisting crack-like discontinuities in these structures, as they can become crack initiation sites. Thus, NDE methods

for FSWs need to provide reliable detection of very tight KB, in addition to detection of LOP and other discontinuities.

Friction Stir Welding

Friction stir welding of butt joints is performed with a rotating pin tool that is thrust into the joint under an axial load. As the metal around the tool heats up, the resistance to deformation of the material is drastically reduced and plasticized metal is readily moved around the tool. This local plastic flow combined with the translational movement of the pin tool along the interface between the abutting surfaces generates a FSW joint. Figure 1 schematically shows the FSW process. Figure 2 is a photomicrograph of a cross-section in a full-penetration FSW, and Figure 3 shows example photomicrographs of (a) a sound FSW, (b) KB and (c) LOP at the back side of FSWs.

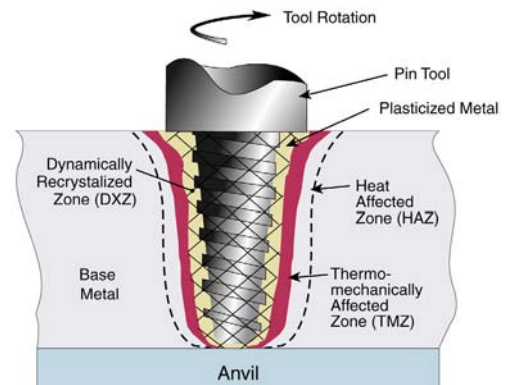


Figure 1. A schematic of the FSW process.

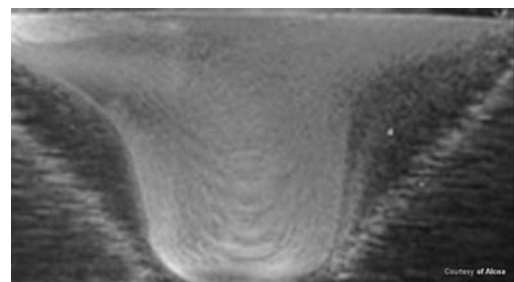
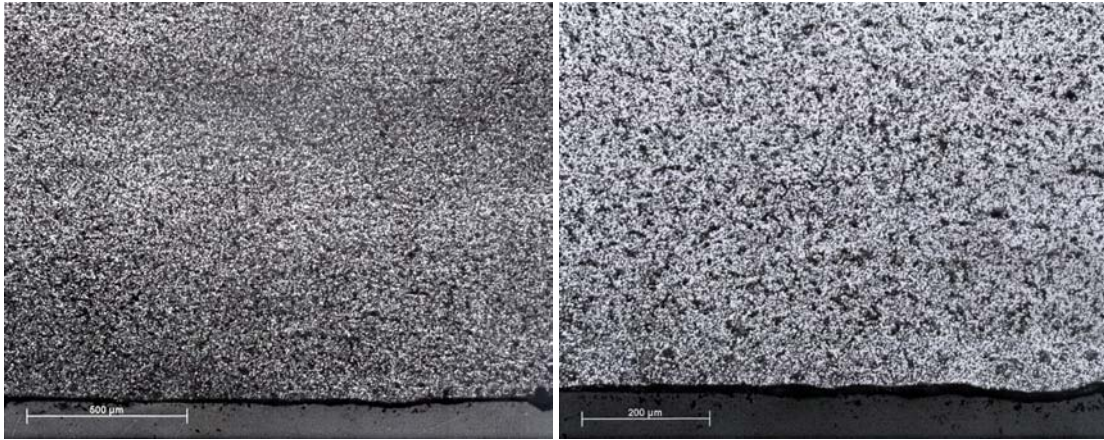
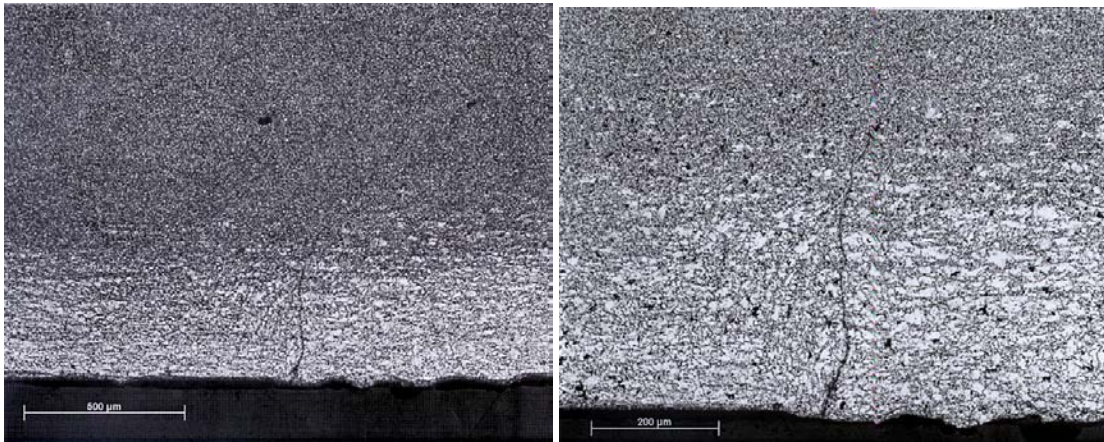


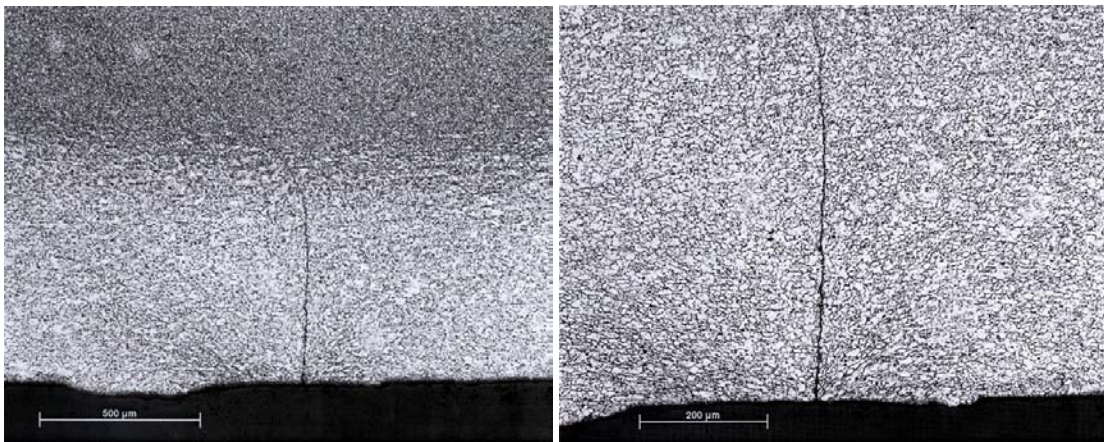
Figure 2. Cross-Sectional macrograph of a full-penetration FSW.



(a) Without discrepant conditions



(b) Kissing Bond



(c) LOP

Figure 3. Photomicrographs of etched cross-sections of butt FSWs near the backside: (a) no discrepant conditions; (b) kissing bond; (c) lack of penetration.

MWM-Array Sensor Evaluation of FSWs

This study focused on the use of MWM-Arrays to detect KB and LOP discontinuities in extrusions joined by the FSW process, in the as-welded condition and after light machining. The methods of using eddy current sensors to map electrical properties of FSWs, were conceived, proven and patented by Goldfine.¹ In particular, Goldfine et al. demonstrated the use of two-dimensional images of eddy current sensor responses (corrected for lift-off variations) as a means for detecting discontinuities relevant to the quality of FSWs and measuring nugget width, and showed correlation of the measured nugget width with LOP depth.^{1,2} Thus, sufficient weld nugget width as measured by eddy current sensors at the back side could be used to ensure a low likelihood of an LOP.

The MWM-Array sensor used in this study (see Figure 4) has 37 sensing elements representing 37 fully parallel channels, and one rectangular drive winding.

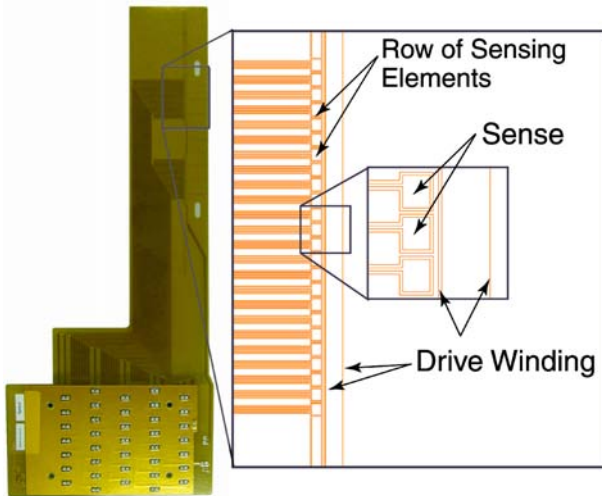


Figure 4. Photograph of the MWM-Array sensor FA57 and detailed schematic that shows some of the sensing elements, including 18 central elements used for scanning in this study.

For the study described here, ALCOA produced several panels with sound FSWs as a control set, and a number of panels with intentional KBs and LOPs at the back side as a test set. The exact locations, depths and lengths of these discontinuities, were carefully established with the help of weld cross-sections and root-bend tests on representative weldments. The actual conditions of the test panels were not provided to JENTEK before MWM-Array scan results were provided to ALCOA.

The discontinuities were produced by selected alteration of FSW tool geometry in conjunction with corresponding adjustment of welding parameters. To inspect for KB and LOP the backside of the FSWs were scanned with the MWM-Array using three different frequencies: 398 kHz, 2 MHz and 10 MHz. This produced electrical conductivity and lift-off images. In order to best represent the electrical conductivity near the back surface of the welds, the MWM-Array measurements were performed at rather high frequencies,

because higher frequencies correspond to shallow penetration of the eddy current sensor fields into aluminum alloys. Prior to scanning, the MWM-Array was calibrated in air, without the use of conductivity standards, as described in ASTM Standard E2338-04⁴. Interestingly, although the resultant images are similar to chemical etching, they are more practical and useful in qualitatively determining the microstructural distribution of the different regions, e.g., DXZ, TMAZ, and HAZ in the FSWs at their back surfaces. Because of the complex geometry of the part, only 18 channels of the available 37 channels were used during scanning. This provided a 0.72-in. (18.3-mm) wide scan path; when needed, either successive scans could be concatenated to form an image, or a single, significantly wider scan can be accomplished with a longer array. Figure 5 shows a photograph of the scanning set-up.

The sensor was scanned in the longitudinal and transverse directions on the anvil-contacting, back surface of the panels, i.e., on the side opposite to the FSW tool. Screen captures from the JENTEK GridStation[®] software displaying conductivity images at 2 MHz for the as-welded condition are shown in Figures 6 through 8. It should be noted that, due to the linear geometry of the MWM-Array drive, eddy currents are induced primarily in the direction parallel to the drive conductors and the resulting MWM conductivity measurements are in this direction as well. Because of this, in the longitudinal scan orientation, the conductivity is measured in the direction perpendicular to the weld, whereas for transverse scans, the conductivity is measured in the direction parallel to the weld.

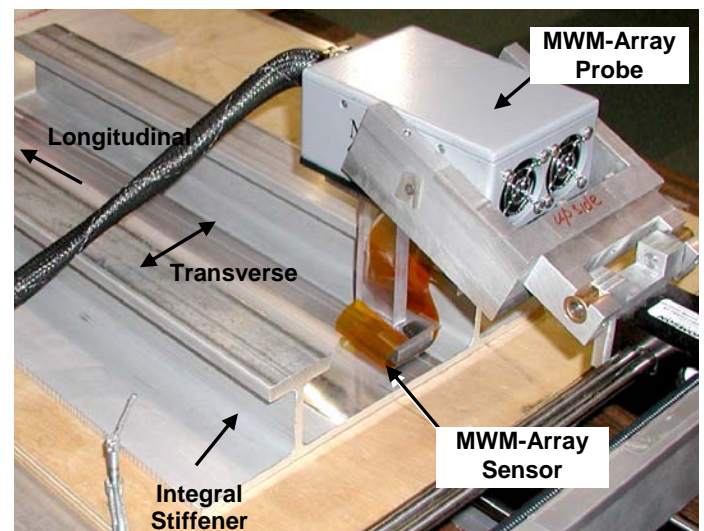


Figure 5. Photograph of the scanning set-up for this study. Note the complex geometry of the extrusions and the ability to scan the region of interest, in spite of close proximity of the tall integral stiffeners.

For transverse scans, the response from the 18 channels is sufficiently similar, and the average of all responses can be plotted (see Figure 9 for a representative plot of conductivity).

Repeat scans of the same FSWs were made to verify repeatability of the conductivity maps (C-scans) from longitudinal scans and conductivity profiles (B-scans).

For all scans, a portion of each scan was acquired on a separate plate of aluminum alloy 6061-T6511. This provided a region of uniform conductivity that was used to normalize the acquired data (removing any channel-to-channel variations not accounted for perfectly by the air calibration). This is the dark region on the left hand side of the conductivity images in Figures 6 through 8 and the cause of the sharp transition at the 55-mm position conductivity in the plot of Figure 9.

The primary difference between the panels with the sound welds (Figure 6) and those containing either or both KB and LOP discontinuities (Figure 7) is the conductivity of the central region of the FSW joint. In the case of the sound welds, this central region represents a wide DXZ that has a relatively low conductivity and is characteristic of full penetration FSWs. The conductivity increases when a KB is present and is yet higher for a weld with an LOP. This increase in conductivity is readily apparent where the transition from a KB to an LOP occurs in Figure 7.

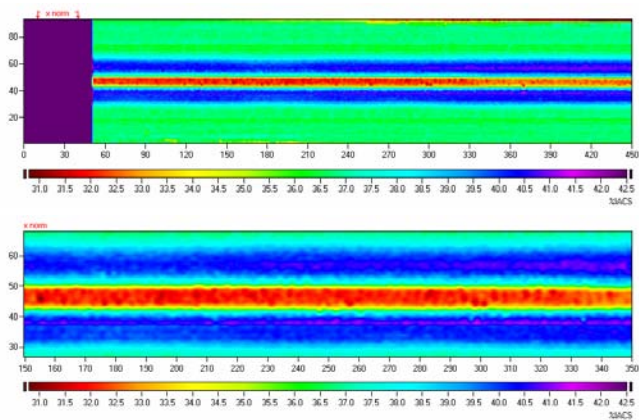


Figure 6. MWM-Array measured conductivity acquired during a longitudinal scan of a panel with a sound FSW, in the as-welded condition. The lower image is an expanded view of the scan showing the FSW central (i.e. mid-width) region highlighting the DXZ (low conductivity area) and TMZ and HAZ (high conductivity areas). The scales of both x and y axes are in millimeters.

The conductivity images capture not only the differences in the FSW central region, but also variability in the higher conductivity TMAZ and HAZ on either side of the DXZ. This latter variability can be caused, for example by changes in the feed rate or rotational speed of the pin tool.

Another feature that is readily detected by this technique is a cracklike planar type discontinuity, that may form when the welding conditions result in a very large LOP. These, often intermittent discontinuities are indicated readily by a sharp

drop in the MWM-Array measured conductivity in the central DXZ region (see Figure 8).

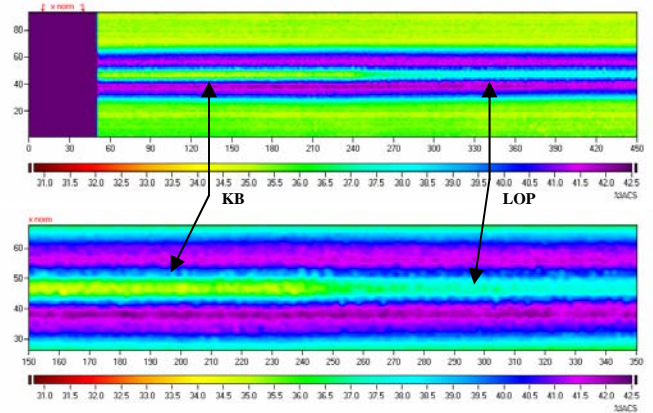


Figure 7. MWM-Array measured conductivity acquired during a longitudinal scan of a panel containing a FSW with both KB (left hand side) and LOP (right hand side) type discontinuities, in the as-welded condition. Notice, in contrast to the sound-weld (Figure 6), the DXZ becomes physically narrower in the KB region and more so in the LOP region while the conductivity increases. In the lower image, an expanded view at the FSW central region shows the transition from KB to LOP occurs at, approximately, 250 mm.

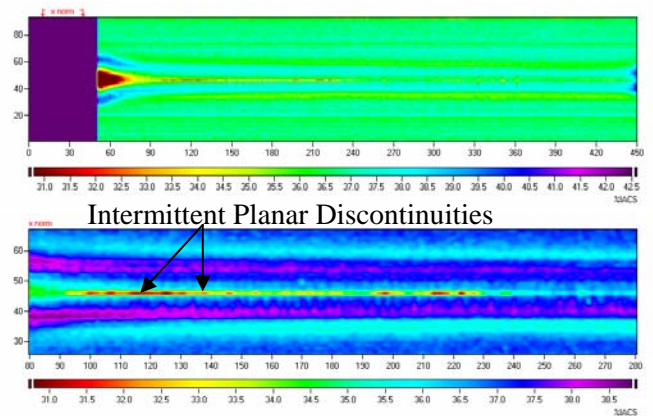


Figure 8. MWM-Array measured conductivity acquired during a longitudinal scan of an FSW panel in the as-welded condition containing an intermittent planar type discontinuity. The bottom image contains an expanded view of the image at the FSW central region-with a rescaled color range to highlight the narrow DXZ and the reduction in conductivity due to the presence of the discontinuity.

This study also investigated the capability of the MWM-Array to provide reliable results after skim-machining a layer off of the back surface. The goal is to remove unacceptable discontinuities, if present, with minimal material removal. Lift-off images from MWM-Array scans at all three frequencies for the skim-machined back surface condition

revealed, as expected, a significant difference in the measured lift-off compared to the as-welded condition (see Figure 10).

Note that the GridStation software uses a physics-based model generated database to convert the MWM-Array response into conductivity and lift-off images¹. These lift-off images are valuable not only for control of sensor performance but also for general examination and characterization of surface conditions (e.g. asperities, pits, etc.). During welding, under sufficient forging force and welding heat input, the anvil can imprint its texture onto the backside of the FSWs. As can be seen in Figure 10, such textures can cause subtle variations in the conductivity measured at the back sides of these welds.

Comparison of transverse scans of panels in both the as-welded and skim-machined conditions shows the most pronounced difference in the conductivity of the HAZ with a lower HAZ conductivity after skim machining for the KB case (see Figure 9).

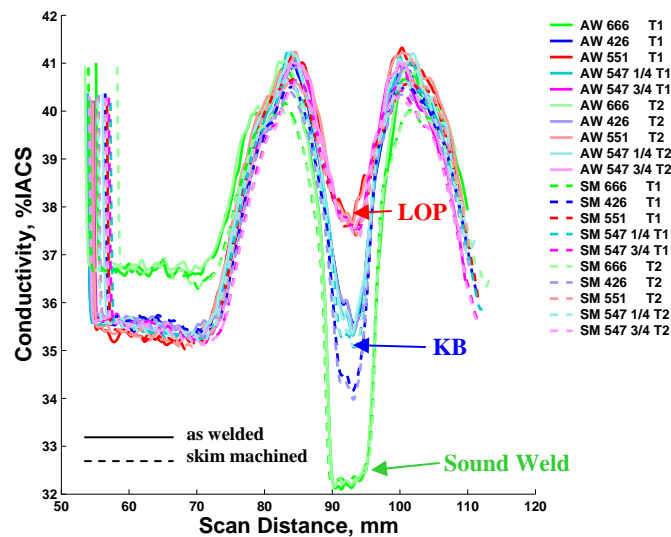


Figure 9. Plots of conductivity acquired during transverse scans of panels in the as-welded (solid lines) and skim-machined (dashed lines) surface conditions. The HAZ peak conductivity for all the panels decreases with skim-machining. The conductivity of the FSW central region for sound welds and welds with LOP change only slightly with machining. The greatest change was observed in the decrease of the FSW central region conductivity for welds with the KB discontinuities.

The data in Figure 9 suggest that the conductivity of the DXZ for sound welds are generally quite similar prior to and after light machining. The same is true for welds with large LOP. However, in the case of panels with KB, a noticeable shift in conductivity after skim machining was observed. As material that was poorly welded is removed and the exposed surface moves towards the weld nugget, the MWM-Array measured conductivity approaches that of a sound weld. It is expected that this trend of conductivity change toward the DXZ conductivity, as the backside is incrementally machined, is

common in the welds with KB and/or LOP discontinuities; but, that for LOP significantly more material must be removed before the conductivity will approach that of a sound weld.

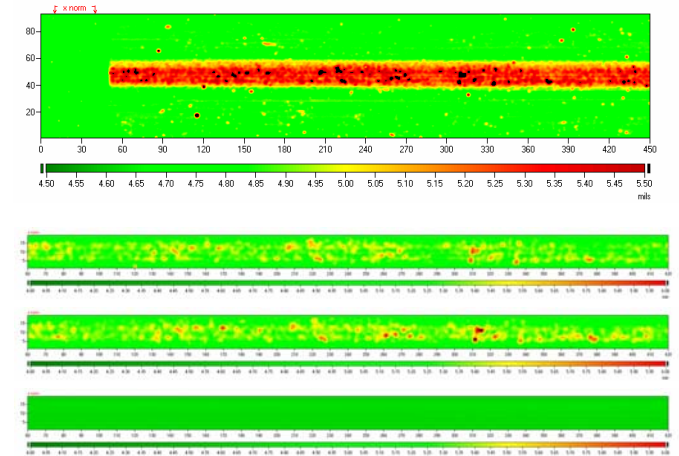


Figure 10. MWM-Array measured lift-off acquired during longitudinal scanning of two different FSW panels. The top two images are from the same scan of a panel with different color scales applied. The bottom two images were acquired from a different panel before and after light machining. In the top image, the anvil imparts a texture to the back surface which results in a slightly higher median lift-off compared to the machined surface on either side of the weld. The center two images show that depressions in the anvil will produce similar patterns of asperities in the backside of successively welded panels.

The conductivity change with depth from the back surface is illustrated well by the MWM-Array “cross-sectional” image shown in Figure 11 where the LOP region conductivity is higher than in DXZ. The image in Figure 11 was obtained by scanning an end-face of a FSW butt welded panel. This figure also shows a visualization of the conductivity/lift-off Measurement Grid (database) used to produce B-scan conductivity profiles and C-scan images¹.

Conclusions

The MWM-Array, eddy current based, technique evaluated in this program is very effective in a) detecting KB, LOP and planar type discontinuities, b) imaging the various microstructural zones, i.e., DXZ, TMAZ, HAZ, and c) mapping the back surfaces of FSWs. These capabilities, which are afforded by imaging of electrical conductivity and lift-off, can make this technique a very useful tool in controlling the FSW process and ensuring the quality (soundness) of the joints. The results clearly show that, for both as-welded and skim-machined surface conditions, the MWM-Array generated information provides an effective discrimination between sound welds and welds that contain discrepant conditions.

Acknowledgements

The authors would like to acknowledge the contribution of their colleagues at JENTEK Sensors, Inc., Kyle L. Williams of the Alcoa Technical Center Alcoa (ATC) who helped to produce the FSW samples and ATC's Alloy-Technology group that provided the metallographic services.

References

- ¹ N. Goldfine, V. Zilberstein, D. Schlicker, D. Grundy, A. Washabaugh, I. Shay, *High Resolution Inductive Sensor Arrays for Material and Defect Characterization of Welds*, U.S. Patent No. 6,727,691, Apr. 27, 2004.
- ² N. Goldfine, Grundy, D., Zilberstein, V., Kinchen, D.G., *Friction Stir Weld Inspection through Conductivity Imaging using Shaped Field MWM®-Arrays*, Proceedings of the 6th International Conference on Trends in Welding, Callaway Gardens, GA; ASM International, January 2003.
- ³ W. Thomas, Nicholas, E., Needham, J., Murch, M., Temple-Smith, P., Dawes, C.: *Friction Stir Butt Welding*, International Patent Appl. No. PCT/GB92/02203 and GB Patent Appl. No. 9125978.8, Dec. 1991, U.S. Patent No. 5,460,317.
- ⁴ ASTM Standard Practice E2338-04, *Characterization of Coatings Using Conformable Eddy-Current Sensors without Coating Reference Standards*, ASTM International, Book of Standards, Vol. 03, 2004.

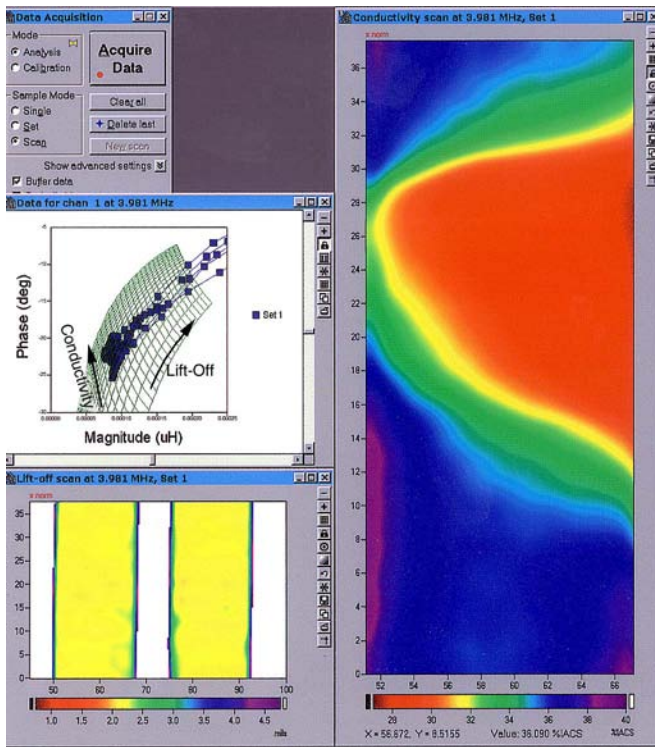


Figure 11. Image of electrical conductivity revealing the nugget, TMZ, HAZ and base metal. The image was generated by scanning an MWM-Array over an end-face of a FSW plate sample, and using the conductivity/lift-off Measurement Grid (precomputed database) to convert the MWM-Array response to conductivity and lift-off at each point in the image¹.